Available online at www.sciencedirect.com
ScienceDirect
Tetrahedron: Asymmetry
Tetrahedron: *Asymmetry* 18 (2007) 1655–1662

Theoretical study on the enantioselective α-amination reaction of 1,3-dicarbonyl compounds catalyzed by a bifunctional-urea

Rongxiu Zhu, Dongju Zhang, Jian Wu and Chengbu Liu*

Institute of Theoretical Chemistry of Shandong University, Jinan 250100, PR China

Received 18 May 2007; accepted 10 July 2007
Available online 7 August 2007

Abstract—The direct catalytic enantioselective α-amination reaction of carbonyl compounds, a powerful approach to asymmetric carbon–nitrogen bond-forming, has been extensively studied, however, our understanding of the mechanism is far from complete. A theoretical study is presented for the α-amination reaction of 2-acetylcyclopentanone with azodicarboxylate catalyzed by a urea-based chiral bifunctional organocatalyst. By performing density functional theory (DFT) calculations, we have identified a detailed mechanism of the reaction and the roles of the amino group and urea in the catalyst. The structures of the catalyst, substrates, intermediates, and transition states involved in the reaction have been located along four possible reaction channels. The rate-determining step is the C–N bond-forming step. The calculations show that the catalyst promotes the reaction by deprotonating 2-acetylcyclopentanone and forming hydrogen bonds with the substrates. The origin of enantioselectivity of the reaction is also discussed.

1. Introduction

Catalytic asymmetric carbon–nitrogen bond-forming processes are of fundamental importance in organic chemistry, as molecules containing this functionality are chiral key elements in many important natural compounds.[1] The direct catalytic enantioselective α-amination of carbonyl compounds represents an appealing approach to an asymmetric carbon center attached to a nitrogen atom, and the development of asymmetric catalysts for such processes has been the focus of recent research efforts.[2–7] Impressive progress has been made recently in the development of bifunctional organic catalysts for enantioselective amination reactions. For example, efficient preparations of enantiomerically pure natural and non-natural α-amino acids, α-amino hydrazides, α-amino carbonyls, and α-amino alcohols have been achieved by using azodicarboxylates as the nitrogen donors[8–10] and L-proline derivatives as organocatalysts. Nonetheless, the development of new catalyst systems with broad substrate scope with respect to both nucleophilic and electrophilic reacting partners remains an important challenge.

Recently, chiral bifunctional-thiourea derivatives have emerged as efficient organocatalysts for different organic transformations.[11] Examples of the enantioselective Strecker synthesis,[12] hydrophosphonylation of imines,[13] acyl-Pictet–Spengler reactions,[14] asymmetry acyl Mannich,[15] and nitro-Mannich[16] reactions, Michael additions,[17–20] Baylis–Hillman reactions,[21,22] and dynamic kinetic resolution of azlactones[23] have been reported. In these reactions, the chiral bifunctional-(thio)ureas have successfully been employed. Despite extensive experimental studies on the bifunctional-(thio)urea catalysis, comprehensive theoretical analyses to elucidate the detailed mechanism of this type of organocatalysis remain few.[24,25]

In a recent experimental study, Takemoto et al.[26] reported bifunctional-urea catalyzed α-amination reactions of cyclic 1,3-dicarbonyl compounds with azodicarboxylate as the nitrogen donor. It was found that the catalyzed reactions gave high enantioselectivity, and the urea moiety of the catalyst played an important role for the high enantioselectivity and reaction rate. However, the origin of the enantioselectivity of the catalyzed reaction, the role of the urea moiety in the catalyst, and the details of the reaction mechanism still remain unclear. As a result, a detailed theoretical study on this catalyzed reaction is highly desirable and worthwhile pursuing.

In previous theoretical studies[24,25] on bifunctional-thio-(urea) catalysis, DFT methods were used to study the mechanism of the catalyzed Michael addition reactions

* Corresponding author. E-mail: cbliu@sdu.edu.cn

0957-4166/$ - see front matter © 2007 Published by Elsevier Ltd.
doi:10.1016/j.tetasy.2007.07.009

between 1,3-dicarbonyl compounds and nitroolefins. The results revealed that the bifunctional-(thio)urea derivatives can activate both nucleophilic and electrophilic substrates through protonating the amino group and forming multiple H-bonds between the catalyst and two substrates, respectively, and that the enantioselectivities of the reactions are related to the binding mode of the two substrates to bifunctional-urea catalyst.

Herein, we report the reaction of cyclic 1,3-dicarbonyl compound 2-acetylcyclopentanone with dimethyl azodicarboxylate catalyzed by a bifunctional-urea catalyst. This reaction is a prototype of catalyzed α-amination for the study (shown in Scheme 1). The aims of this research are (a) to gain a better understanding of the activity and selectivity of the bifunctional catalyst and (b) to shed light on the mechanism details of this reaction and hence obtain a better interplay between theory and experiment.

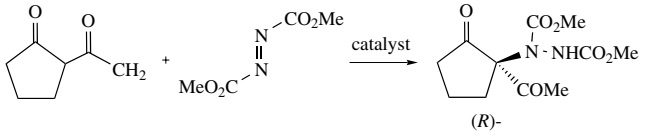

Scheme 1. Urea-catalyzed enantioselective α-amination of 2-acetylcyclopentanone with dimethyl azodicarboxylate.

2. Models and computational details

The bifunctional-urea catalyst was modeled by a simple molecule (denoted as **cat.**) that involves the essential structural feature of the catalyst (see Fig. 1). This catalyst model is analogous to that used in our previous study.[25] All calculations were performed with the GAUSSIAN03 software package[27] under the framework of DFT. The B3LYP functional[28–30] was chosen in view of its effective performance for the systems involving organic compounds. At the B3LYP/6-31G(d) level, the stationary points on the potential energy surface (PES) have been located by full geometry optimization without any symmetric restriction and their nature (local minima or first-order saddle points) was characterized by performing vibrational frequency calculations. The intrinsic reaction coordinate (IRC) pathways have been traced in order to verify two desired minima connected by the transition states. To obtain accurate energetics, we performed additional single-point energy calculations, using a more extended 6-311++G(d,p) basis set on all atoms. Unless stated otherwise in the text, the relative energies reported herein are those obtained from the B3LYP/6-311++G(d,p)//B3LYP/6-31G(d) calculations. For all cited energies, the ZPE corrections have been included.

Solvent effects have been considered at the same DFT level by re-optimizing the structures obtained in gas-phase using a self-consistent reaction field (SCRF) method,[31–33] based on the polarizable continuum model (PCM)[34–36] and using UAKS cavities.[37] The dielectric constant of toluene was taken as 2.38.

3. Results and discussion

3.1. Structures of catalyst and 2-acetylcyclopentanone

As demonstrated in the experimental[17b] and theoretical[24] studies, the bifunctional-(thio)urea catalyst is characterized by two N–H bonds of (thio)urea and the amino group oriented in the same direction, thus an intramolecular N–H···N hydrogen bond can be formed between the tertiary amine and neighboring N–H group. The optimized structure of the model catalyst is presented in Figure 1. The calculated distance of N–H···N hydrogen bond is 2.22 Å, which is similar to the value reported by Hamza (2.15 Å).[24]

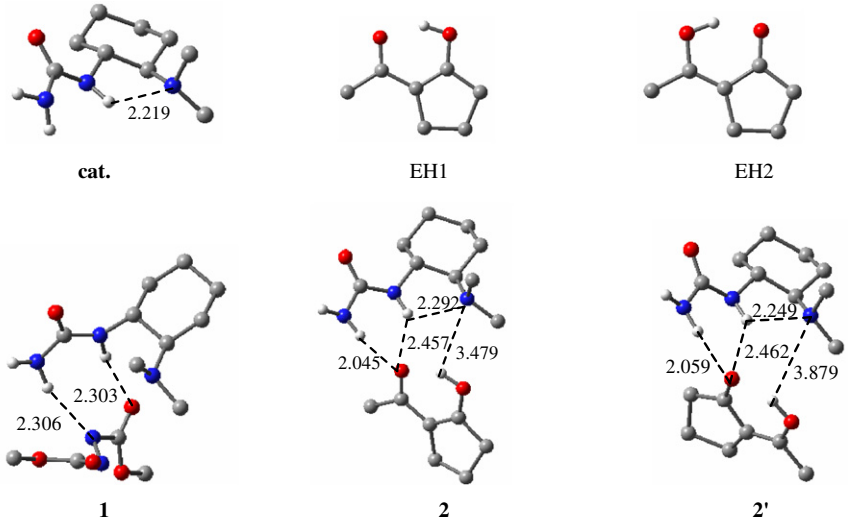

Figure 1. Optimized structures of the catalyst, substrates, and catalyst–substrate complexes. The hydrogen atoms on the rings and methyl groups are omitted for clarity.

2-Acetylcyclopentanone is a cyclic β-diketone that exists as keto- and enol-tautomers in equilibrium, as shown in Scheme 2, where KH and EH represent the keto and enol tautomeric forms of 2-acetylcyclopentanone, respectively. Since the enol tautomers of 2-acetylcyclopentanone are stabilized by intramolecular hydrogen bonds, EH isomers are the predominant forms in apolar solvents.[38] Two structural isomers were found for EH: one with the hydrogen atom bonded to the cyclic carbonyl oxygen (denoted as EH1) and the other to the side chain carbonyl oxygen (denoted as EH2). The energies of these two structures differ by 1.10 kcal mol^{-1}, EH1 being the less stable. Since the energy barrier related to EH1→EH2 transition is rather low (0.25 kcal mol^{-1}), these two enol tautomers are competitive structures of 2-acetylcyclopentanone for the catalyzed α-amination reaction. Our calculated results indicate that EH1 and EH2 have a similar reaction mechanism, thus in this study EH1 have been thoroughly discussed. Figure 1 shows the optimized structures of EH1 and EH2.

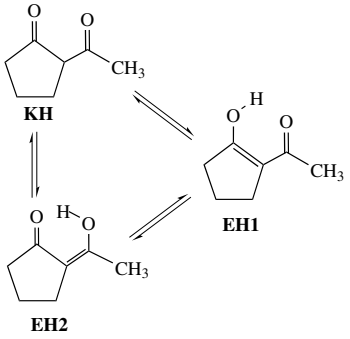

Scheme 2. Keto–enol equilibria of 2-acetylcyclopentanone.

3.2. Mechanism of the bifunctional-urea catalyzed α-amination reaction

From the computational results it follows that the bifunctional-urea catalyzed α-amination reaction involves five major steps: (1) the coordination of the substrate to the catalyst, (2) the protonation of the catalyst to form a catalyst–enolate ion pair, (3) the complexation of dimethyl azodicarboxylate to the ion pair via H-bonds to give a new ternary complex, (4) the formation of the C–N bond; and (5) the proton transfer from the protonated amino group to another nitrogen atom of dimethyl azodicarboxylate, followed by the dissociation of the H-bonded complex to give products and the catalyst. The detailed discussion of the mechanism and the calculated energetics for the catalytic amination reaction of EH1 is presented in the following subsections.

3.2.1. Substrate binding and catalyst protonation. It is expected that both dimethyl azodicarboxylate and 2-acetylcyclopentanone can coordinate with the catalyst via a double H-bond. We searched several possible binary catalyst–substrate complexes and optimized their structures, as depicted in Figure 1.

In complex **1**, dimethyl azodicarboxylate forms a bidentate H-bond with the urea moiety of the catalyst, and the calculated substrate binding energy is only 1.75 kcal mol^{-1}. For the coordination of EH1 with the catalyst, a loose structure, denoted as **2**, is obtained, in which double N–H···O hydrogen bonds are formed and the intramolecular N–H···N hydrogen bond of the catalyst is slightly weakened, as indicated by the structural parameters shown in Figure 1. The calculated binding energy is 4.43 kcal mol^{-1}. However, this structure is not favorable for the proton transfer from the coordinated enol to the amine group of the catalyst, due to the larger distance between these two units. It can be converted into a tight complex **3**, where the coordinated enol and the amino group have reached a proper distance. In structure **3**, the O–H···N hydrogen bond shortens from 3.479 to 1.890 Å, while one of the hydrogen bonds between the urea moiety and the coordinated enol shortens from 2.457 to 1.890 Å, while the other H-bond between the urea and enol elongates from 2.045 to 3.289 Å, and the intramolecular N–H···N hydrogen bond of the catalyst stretches to 2.950 Å. Compound **3** is 3.63 kcal mol^{-1} less stable compared to **2**.

Once the tight binary complex is formed, the protonation process from the coordinated enol to the amine group of the catalyst can take place easily, as the energy barrier related to the **3**→**4** transition is rather low (0.28 kcal mol^{-1}). The resulting ion pair **4** is stabilized via multiple N–H···O bonds that involve the cationic amine moiety and one of the N–H groups of urea moiety as well. Compound **4** is predicted to be 0.21 kcal mol^{-1}, which is more stable than **3**. As seen in Figure 2, the N–H groups of the catalyst

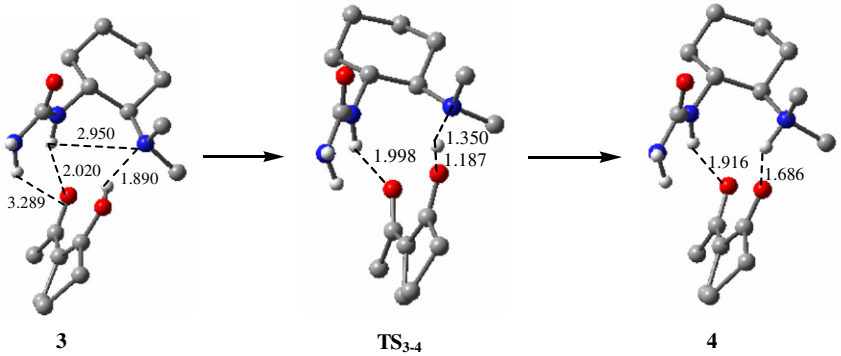

Figure 2. Optimized structures of stationary points located for the protonation process between the catalyst and EH1. The hydrogen atoms on the rings and methyl groups are omitted for clarity.

play an important role in the deprotonation of EH1, because they provide a binding site for EH1 in the near proximity of the tertiary amine and also stabilize enolate **4** via N–H···O hydrogen bonds.

The above results show that not only the binding energy of dimethyl azodicarboxylate to the catalyst is less than that of EH1, but also enolate **4** originated from **2** is more reactive. In addition, we also tried to describe the deprotonation of EH1 in the presence of H-bonded dimethyl azodicarboxylate, however, our attempt was unsuccessful. The optimization calculations always result in a loose-binding catalyst–dimethyl azodicarboxylate–EH1 ternary complex, where the enolate hydrogen atom is too far from the amino group to transfer. As a result, the catalyzed amination reaction is believed to start from the initial binary catalyst–EH complex.

3.2.2. Dimethyl azodicarboxylate–catalyst–enolate ternary complexes. Dimethyl azodicarboxylate can approach **4** from different orientations forming two ternary complexes, denoted as **5a** and **5b**, which control the stereochemical outcome of the reaction. The structures of these two ternary complexes are presented in Figure 3.

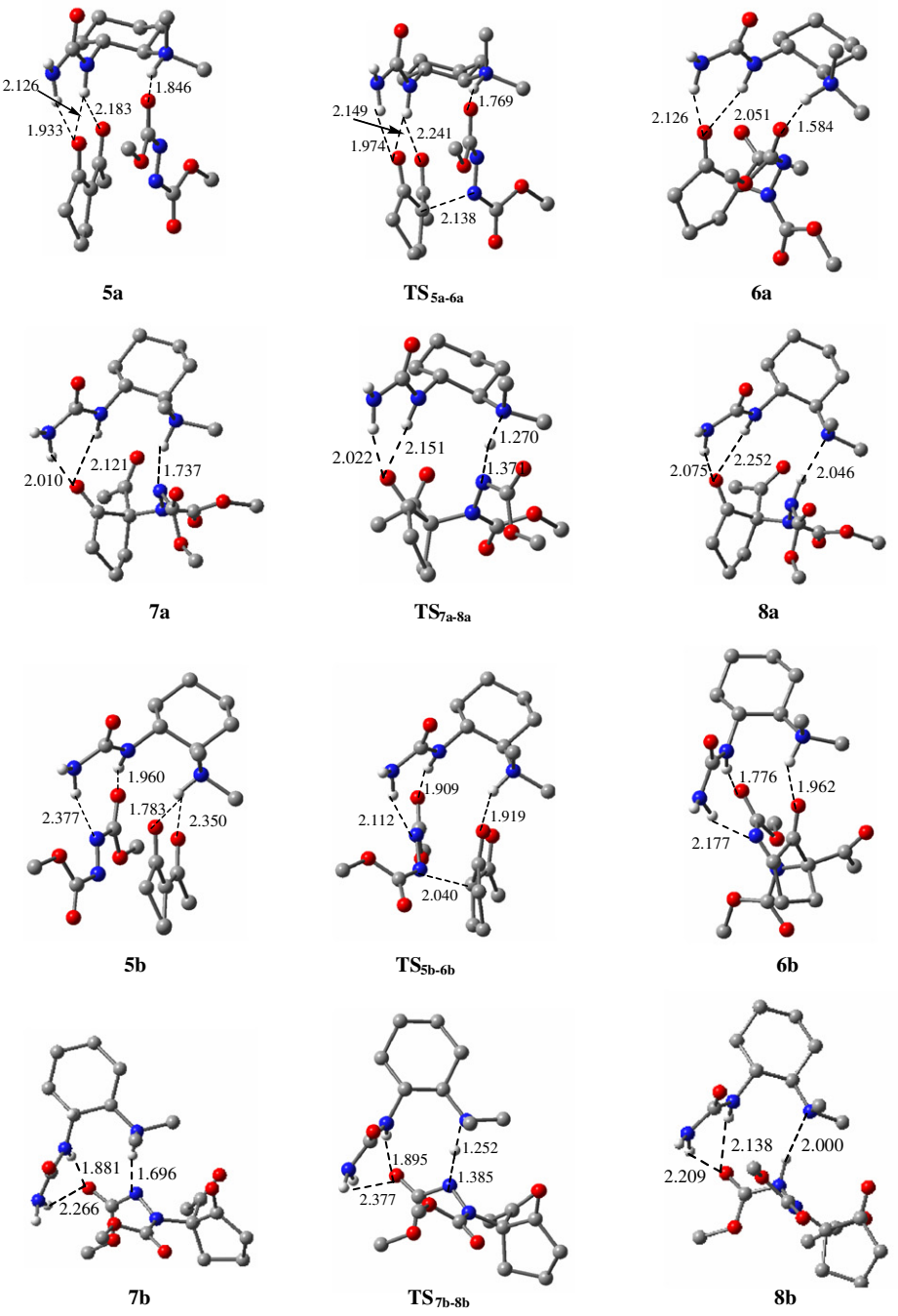

Figure 3. Optimized structures and selected geometric parameters of the stationary points located along channels **A** and **B**. The hydrogen atoms on the rings and methyl groups are omitted for clarity.

In **5a**, dimethyl azodicarboxylate binds to the protonated amine group via the N–H···O H-bond, thus the enolate ion has been pushed to the urea moiety of the catalyst and attached to urea via multiple H-bonds. In contrast, in **5b**, dimethyl azodicarboxylate binds to the urea moiety of the catalyst via double H-bonds and the enolate ion has been pushed to the protonated amine group. The binding energies of dimethyl azodicarboxylate are calculated to be 0.82 kcal mol^{-1} for **5a** and 1.44 kcal mol^{-1} for **5b**.

3.2.3. Two reaction channels for the catalyzed C–N bond-forming reaction. Two different channels (denoted as **A** and **B**) for the catalytic amination reaction of EH1 have been located (see Scheme 3), which start from **5a** and **5b**, respectively. Channel **A** gives an (*R*)-configuration product, while channel **B** yields (*S*)-configuration product. The structures of the intermediates and transition states involved in these two channels are shown in Figure 3, and the calculated energetic profiles are given in Figure 4.

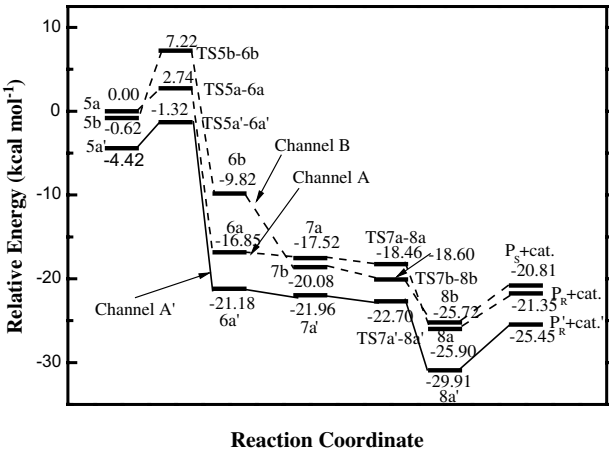

Figure 4. Calculated energetic profiles of channels **A** and **B** along the reaction coordinate, where **A**′ denotes the process of channel **A** in toluene.

Along channel **A**, the nucleophilic center of the enolate anion attacks the electron-deficient dimethyl azodicarboxylate via transition state $\mathbf{TS_{5a–6a}}$ with a very low barrier of 2.74 kcal mol^{-1}, to give adduct intermediate **6a**. The structure of $\mathbf{TS_{5a–6a}}$ indicates that the formation of the C–N bond is coupled with the weakening of the catalyst–enolate interaction, which is due to charge transfer occurring from the anionic enolate to dimethyl azodicarboxylate. Also as a result of negative charge delocalization, the H-bonded linkage between dimethyl azodicarboxylate and the catalyst is strengthened. The changes are also encountered in **6a**, and the result is that **6a** lies 16.85 kcal mol^{-1} below **5a**.

After the C–N bond is formed, the next step is the proton transfer from the protonated amino group to dimethyl azodicarboxylate to yield the catalyst–product complexes, followed by the dissociation of the H-bonded complexes to complete the catalytic cycle. Our calculations indicate that **6a** can rearrange into structure **7a**, where the hydrogen bond between catalyst and dimethyl azodicarboxylate is N–H···N rather than N–H···O. Compound **7a** is only 0.67 kcal mol^{-1}, which is more stable than **6a**. Subsequently, the direct proton shift from catalyst to dimethyl azodicarboxylate yields intermediate **8a** via saddle point $\mathbf{TS_{7a–8a}}$. Compound **8a** is 8.38 kcal mol^{-1} more stable than **7a**. Our computed results show that the relative energy of $\mathbf{TS_{7a–8a}}$ is even below **7a** after ZPE corrections, indicating that proton transfer involves no activation barrier and is exothermic. Finally, the hydrogen bonds in **8a** break to form product P_R along with the catalyst.

In channel **B**, the nucleophilic enolate adds to electron-deficient dimethyl azodicarboxylate, giving adduct **6b**. This step proceeds via transition state $\mathbf{TS_{5b–6b}}$, with a barrier

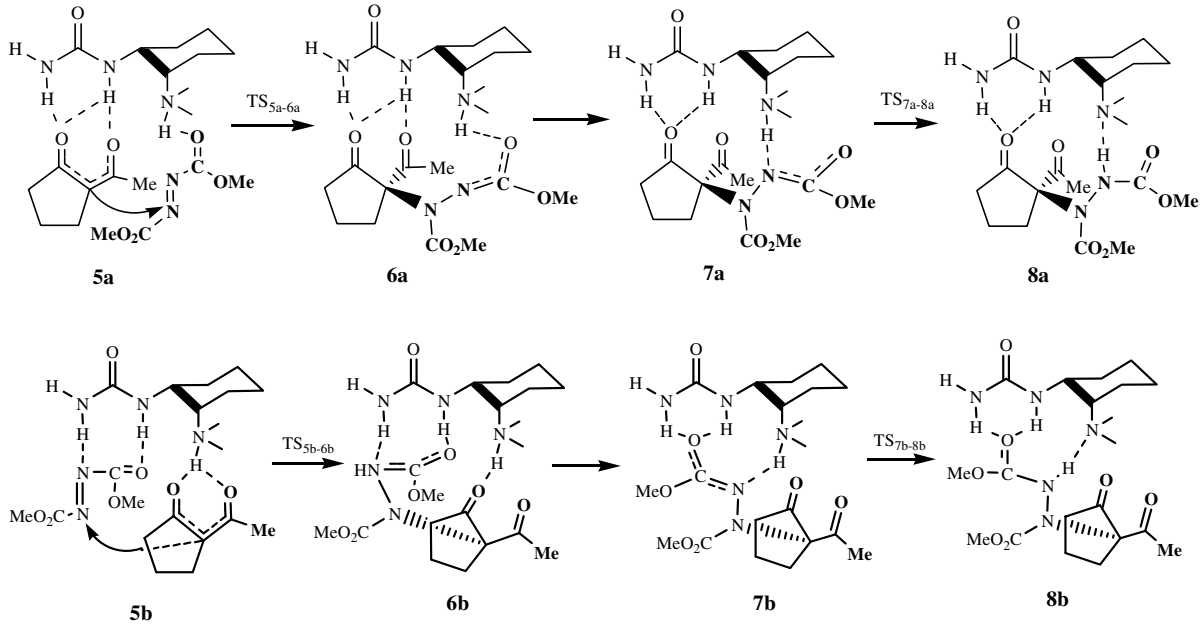

Scheme 3. Two reaction channels proposed for the catalytic α-amination of EH1.

of 7.84 kcal mol^{-1}, lying 9.20 kcal mol^{-1} lower in energy than **5b**. This process is also accompanied by structural changes characteristic of intermolecular charge transfer between the reacting species. From the structure of $\mathbf{TS_{5b-6b}}$, one can see that the urea–dimethyl azodicarboxylate interaction becomes apparently stronger along the reaction coordinate, whereas the H-bonded linkage between the enolate carbonyl and the protonated amino group is weakened.

Subsequently, **6b** is converted into another hydrogen bonding (NH···N) complex **7b**; compound **7b** is 8.77 kcal mol^{-1}, which is more stable compared to **6b**. Proton transfer from the catalyst to nitrogen atom of dimethyl azodicarboxylate yields intermediate **8b** via saddle point $\mathbf{TS_{7b-8b}}$. Compound **8b** is 7.12 kcal mol^{-1}, which is more stable than **7b**. Our computed results show that the relative energy of $\mathbf{TS_{7b-8b}}$ is also below **7b** after ZPE corrections, indicating that proton transfer in channel **B** is no activation barrier and exothermic. Finally, the hydrogen bonds in **8b** break to form product P_S along with the catalyst.

From the above analyses, channel **A** is energetically more favorable compared to channel B. From the calculated barriers, it is clear that the C–N bond formation is the stereocontrolling and the rate-determining step of the reaction.

3.2.4. Catalytic amination reactions involving EH2. Similar to the investigation for EH1, we briefly studied the catalytic amination reactions of EH2. It was expected that EH2 has the same reaction mechanisms with EH1. First, EH2 coordinates to the catalyst, followed by the protonation of the catalyst to give reactive enolate **4′** (**2′** → **3′** → $\mathbf{TS_{3'-4'}}$ → **4′**) (see Fig. 5). The energy barrier related to the **3′**→**4′** transition is 0.37 kcal mol^{-1}, and the whole process is slightly exothermic (0.16 kcal mol^{-1} compared to **2′**). Then dimethyl azodicarboxylate coordinates to **4′** from the different orientations to form two ternary complexes (**5c** and **5d**). Starting with these two ternary complexes, two reaction channels, channels **C** and **D**, which correspond to channels **A** and **B** discussed above, respectively, have been considered. The calculations show that (*R*)-configuration and (*S*)-configuration products are obtained along channels **C** and **D**, respectively, which involve three minima and two saddle points (Fig. 6). The barrier of the rate-determining step is predicted to be 4.97 kcal mol^{-1} along channel **C** and 6.66 kcal mol^{-1} along channel **D**.

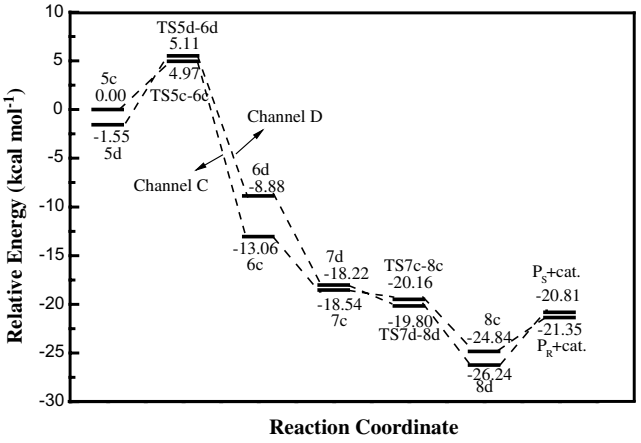

Figure 6. Calculated energetic profiles for the catalytic amination reactions of EH2 along the reaction coordinate.

Taken together, there are four channels for the urea-catalyzed amination reaction. By comparison of these four reaction channels, channel **A**, which gives an (*R*)-configuration product, is the most favorable for the catalytic enantioselective amination reaction. To evaluate the solvent effects on this reaction, the PCM model (toluene solvent) was applied for the stationary points along the most favorable channel. The calculated results show that solvent effects systemically stabilize all the species in about 4.3 kcal mol^{-1}, as shown by the PES profile drawn out using a solid line in Figure 4 (denoted as channel **A′**). Clearly, the PES profile along channel **A** from the PCM model is very similar to that from the gas-phase model. Thus, we believe that the gas-phase model is able to describe the real toluene-mediated system.

3.3. Enantioselectivity

The last issue investigated in this study concerns the observed enantioselectivity of the reaction. Free energy results allow us to predict, at least on a qualitative basis, the outcome of a reaction that might yield different products as a consequence of the existence of two or more reaction channels. In our calculations, the ee is defined as ([R] − [S])/([R] + [S]) and [R]/[S] is obtained by the ratio between the combined rates of channels **A** and **C** and the combined rates of channels **B** and **D**, where [R] and [S]

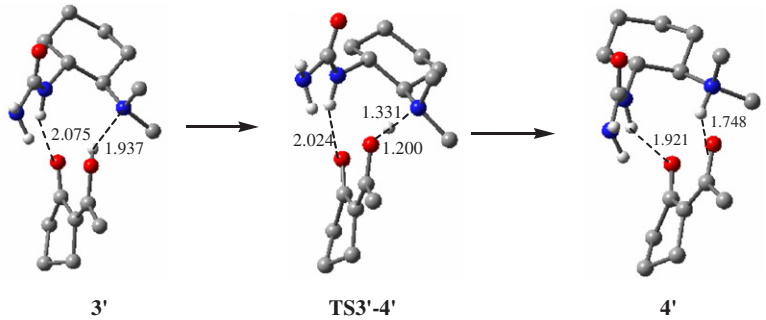

Figure 5. Optimized structures of stationary points located for the protonation process between the catalyst and EH2. The hydrogen atoms on the rings and methyl groups are omitted for clarity.

are the concentrations of the two enantiomers. The temperature dependent pre-exponential factor is simplified, and only the exponential parts are retained

$$\frac{[R]}{[S]} = \frac{\exp(-G^{\neq}_{R(a)}/RT) + \exp(-G^{\neq}_{R(c)}/RT)}{\exp(-G^{\neq}_{S(b)}/RT) + \exp(-G^{\neq}_{S(d)}/RT)} \quad (1)$$

The enantiomeric excess can be calculated as follows:

$$\text{ee } \% = \frac{[R]-[S]}{[R]+[S]} \cdot 100 = \frac{\frac{[R]}{[S]}-1}{\frac{[R]}{[S]}+1} \cdot 100 \quad (2)$$

The relative free energies (298 K) of channels **A**, **B**, **C**, and **D** are 3.26, 8.54, 4.99 and 7.61 kcal mol^{-1}, respectively. Application of Eqs. 1 and 2 provided an enantiomeric excess of 99.8% ee. Compared to the experimentally observed value (~80% ee), this result seems to be overestimated, however, it does provide the correct indication of the stereochemical preference of the reaction.

4. Conclusion

The bifunctional-urea catalyzed enantioselective α-amination reaction of 1,3-dicarbonyl compounds with azodicarboxylate has been investigated by performing DFT calculations. The predicted mechanism involves initial nucleophile activation via protonation of the amino group and electrophile activation through substrate binding to urea; then C–N bond formation between these two activated components; and finally, the proton transfer from the protonated amino group to adduct, followed by the dissociation of the H-bonded complex to give amination product along with the catalyst. Four reaction channels, corresponding to the different coordinate modes of two isomers of EH and dimethyl azodicarboxylate to the catalyst, have been characterized in detail. It has been found that the enantioselectivity of the reaction is controlled by the C–N bond-forming step, which is the rate-determining step. Our calculated results confirm that the urea moiety of the catalyst has a significant effect on the reaction. The present DFT study well explains the experimental findings and provides the details of the mechanism.

Acknowledgments

This work was supported by the National Natural Science Foundation of China (Nos.: 20473047, 20503014, and 20633060) and the Major State Basic Research Development Program of China (No. 2004CB719902). We thank the High Performance Computational Center of Shandong University for computer resources.

References

1. Williams, R. M. *Synthesis of Optically Active α-Amino Acids*; Pergamon: Oxford, 1989.
2. Evans, D. A.; Nelson, S. G. *J. Am. Chem. Soc.* **1997**, *119*, 6452–6453.
3. Kobayashi, S.; Yamashita, Y.; Ishitani, H. *Chem. Lett.* **1999**, 307–308.
4. Yamashita, Y.; Ishitani, H.; Kabayashi, S. *Can. J. Chem.* **2000**, *78*, 666–672.
5. Evans, D. A.; Johnson, D. S. *Org. Lett.* **1999**, *1*, 595–598.
6. Evans, D. A.; Miller, S. J.; Lectka, T.; von Matt, P. *J. Am. Chem. Soc.* **1999**, *121*, 7559–7573.
7. Juhl, K.; Jørgensen, K. A. *J. Am. Chem. Soc.* **2002**, *124*, 2420–2421.
8. Bøgevig, A.; Juhl, K.; Kumaragurubaran, N.; Zhuang, W.; Jørgensen, K. A. *Angew. Chem., Int. Ed.* **2002**, *41*, 1790–1793.
9. List, B. *J. Am. Chem. Soc.* **2002**, *124*, 5656–5657.
10. Kumaragurubaran, N.; Juhl, K.; Zhuang, W.; Bøgevig, A.; Jørgensen, K. A. *J. Am. Chem. Soc.* **2002**, *124*, 6254–6255.
11. For a review, see: Connon, S. J. *Chem. Eur. J.* **2006**, *12*, 5418–5427.
12. (a) Sigman, M. S.; Jacobsen, E. N. *J. Am. Chem. Soc.* **1998**, *120*, 4901–4902; (b) Sigman, M. S.; Vachal, P.; Jacobsen, E. N. *Angew. Chem.* **2000**, *112*, 1336–1338; . *Angew. Chem., Int. Ed.* **2000**, *39*, 1279–1281; (c) Vachal, P.; Jacobsen, E. N. *J. Am. Chem. Soc.* **2002**, *124*, 10012–10014; (d) Tsogoeva, S. B.; Hateley, M. J.; Yalalov, D. A.; Meindl, K.; Weckbecker, C.; Huthmacher, K. *Bioorganic and Medicinal Chemistry* **2005**, *13*, 5680–5685.
13. Joly, G. D.; Jacobsen, E. N. *J. Am. Chem. Soc.* **2004**, *126*, 4102–4103.
14. Taylor, M. S.; Jacobsen, E. N. *J. Am. Chem. Soc.* **2004**, *126*, 10558–10559.
15. Taylor, M. S.; Torunaga, N.; Jacobsen, E. N. *Angew. Chem.* **2005**, *117*, 6858–6862; *Angew. Chem., Int. Ed.* **2005**, *44*, 6700–6704.
16. Yoon, T. P.; Jacobsen, E. N. *Angew. Chem.* **2005**, *117*, 470–472; *Angew. Chem., Int. Ed.* **2005**, *44*, 466–468.
17. (a) Okino, T.; Hoashi, Y.; Takemoto, Y. *J. Am. Chem. Soc.* **2003**, *125*, 12672–12673; (b) Okino, T.; Hoashi, Y.; Furukawa, T.; Xu, X.; Takemoto, Y. *J. Am. Chem. Soc.* **2005**, *127*, 119–125; (c) Hoashi, Y.; Okino, T.; Takemoto, Y. *Angew. Chem.* **2005**, *117*, 4100; *Angew. Chem., Int. Ed.* **2005**, *44*, 4032–4035.
18. Li, H.; Wang, Y.; Tang, L.; Deng, L. *J. Am. Chem. Soc.* **2004**, *126*, 9906–9907.
19. Wang, W.; Wang, J.; Li, H. *Angew. Chem.* **2005**, *117*, 1393–1395; *Angew. Chem., Int. Ed.* **2005**, *44*, 1369–1371.
20. (a) Cobb, A. J. A.; Longbottom, D. A.; Shaw, D. M.; Ley, S. V. *Chem. Commun.* **2004**, 1808–1809; (b) Mitchell, C. E. T.; Cobb, A. J. A.; Ley, S. V. *Synlett* **2005**, 611–614; (c) Cobb, A. J. A.; Shaw, D. M.; Longbottom, D. A.; Gold, J. B.; Ley, S. V. *Org. Biomol. Chem.* **2005**, *3*, 84–96.
21. Maher, D. J.; Connon, S. J. *Tetrahedron Lett.* **2004**, *45*, 1301–1305.
22. Sohtome, Y.; Tanatani, A.; Hashimoto, Y.; Nagasawa, K. *Tetrahedron Lett.* **2004**, *45*, 5589–5592.
23. (a) Berkessel, A.; Cleemann, F.; Mukherjee, S.; Müller, T. N.; Lex, J. *Angew. Chem.* **2005**, *117*, 817–821; *Angew. Chem., Int. Ed.* **2005**, *44*, 807–811; (b) Berkessel, A.; Mukherjee, S.; Cleemann, F.; Müller, T. N.; Lex, J. *Chem. Commun.* **2005**, 1898–1900.
24. Hamza, A.; Schubert, G.; Soós, T.; Ppai, I. *J. Am. Chem. Soc.* **2006**, *128*, 13151–13160.
25. Zhu, R. X.; Zhang, D. J.; Wu, J.; Liu, C. B. *Tetrahedron: Asymmetry* **2006**, *17*, 1611–1616.
26. Xu, X.; Yabuta, T.; Yuan, P.; Takemoto, Y. *Synlett* **2006**, *1*, 137–140.
27. Frisch, M. J.; Trucks, G. W.; Schlegel, H. B.; Scuseria, G. E.; Robb, M. A.; Cheeseman, J. R.; Montgomery, J. A., Jr.; Vreven, T.; Kudin, K. N.; Burant, J. C.; Millam, J. M.; Iyengar, S. S.; Tomasi, J.; Barone, V.; Mennucci, B.; Cossi, M.; Scalmani, G.; Rega, N.; Petersson, G. A.; Nakatsuji, H.;

Hada, M.; Ehara, M.; Toyota, K.; Fukuda, R.; Hasegawa, J.; Ishida, M.; Nakajima, T.; Honda, Y.; Kitao, O.; Nakai, H.; Klene, M.; Li, X.; Knox, J. E.; Hratchian, H. P.; Cross, J. B.; Adamo, C.; Jaramillo, J.; Gomperts, R.; Stratmann, R. E.; Yazyev, O.; Austin, A. J.; Cammi, R.; Pomelli, C.; Ochterski, J. W.; Ayala, P. Y.; Morokuma, K.; Voth, G. A.; Salvador, P.; Dannenberg, J. J.; Zakrzewski, V. G.; Dapprich, S.; Daniels, A. D.; Strain, M. C.; Farkas, O.; Malick, D. K.; Rabuck, A. D.; Raghavachari, K.; Foresman, J. B.; Ortiz, J. V.; Cui, Q.; Baboul, A. G.; Clifford, S.; Cioslowski, J.; Stefanov, B. B.; Liu, G.; Liashenko, A.; Piskorz, P.; Komaromi, I.; Martin, R. L.; Fox, D. J.; Keith, T.; Al-Laham, M. A.; Peng, C. Y.; Nanayakkara, A.; Challacombe, M.; Gill, P. M. W.; Johnson, B.; Chen, W.; Wong, M. W.; Gonzalez, C.; Pople, J. A. GAUSSIAN*03, Revision B05*; Gaussian: Pittsburgh, PA, 2003.
28. Becke, A. D. J. *Chem. Phys.* **1993**, *98*, 1372–1377.
29. Becke, A. D. *J. Chem. Phys.* **1993**, *98*, 5648–5652.
30. Lee, C.; Yang, W.; Parr, R. G. *Phys. Rev. B* **1988**, *37*, 785–789.
31. Tapia, O. *J. Math. Chem.* **1992**, *10*, 139–181.
32. Tomasi, J.; Persico, M. *Chem. Rev.* **1994**, *94*, 2027–2094.
33. Simkin, B. Y.; Sheikhet, I. *Quantum Chemical and Statistical Theory of Solutions—A Computational Approach*; Ellis Horwood: London, 1995.
34. Cances, E.; Mennunci, B.; Tomasi, J. *Chem. Phys.* **1997**, *107*, 3032–3041.
35. Cossi, M.; Barone, V.; Cammi, R.; Tomasi, J. *Chem. Phys. Lett.* **1996**, *255*, 327–335.
36. Barone, V.; Cossi, M.; Tomasi, J. *J. Comput. Chem.* **1998**, *19*, 404–407.
37. Takano, Y.; Houk, K. N. *J. Chem. Theory Comput.* **2005**, *1*, 70–77.
38. Iglesias, E. *New J. Chem.* **2002**, *26*, 1352–1359.